Investigation of Iron−Sulfur Covalency in Rubredoxins and a Model System Using Sulfur K-Edge X-ray Absorption Spectroscopy

Kendra Rose,[†] Susan E. Shadle,[†] Marly K. Eidsness,[‡] Donald M. Kurtz, Jr.,[‡] Robert A. Scott,[‡] Britt Hedman,*[,§] Keith O. Hodgson,*[,†,§] and Edward I. Solomon*[,†]

Contribution from the Department of Chemistry, Stanford University, Stanford, California 94305, Department of Chemistry and Center for Metalloenzyme Studies, University of Georgia, Athens, Georgia 30602, and Stanford Synchrotron Radiation Laboratory, Stanford University, Stanford, California 94309

Received April 20, 1998. Revised Manuscript Received August 20, 1998

Abstract: X-ray absorption spectroscopy at the sulfur K-edge at ∼2470 eV has been applied to a series of mononuclear iron−sulfur complexes to determine the covalency and its distribution over the ligand field split d-orbitals. A comparison is made between the S K-edges of a model and three different rubredoxin proteins to define the changes in covalency upon incorporation of the site into the protein. It is found that the covalency decreases in the proteins relative to the model. The thiolate−Fe(III) bond in these systems is highly covalent, and a modulation of this covalency in the proteins can contribute to the redox properties of the active site. It is determined that, while the hydrogen bonding effects seem to influence covalency, there is not a direct correlation between the change in covalency, the number of hydrogen bonds, and the redox potentials of these sites.

Introduction

Metalloproteins containing iron−sulfur active sites are present in all forms of life and are very commonly involved in electron transfer. Rubredoxins are the simplest of the Fe−S proteins, and most have molecular weights that are usually in the range of 6−7 kD. The Fe site found in rubredoxins contains a single iron ion bound by four thiolates from cysteine residues in a nearly T_d geometry.[1,2] The biologically relevant redox reaction of rubredoxins involves a one-electron Fe(II)/Fe(III) couple. The reduction potentials of various rubredoxin proteins range from −60 to +5 mV vs SHE, while those of model complexes are in the region around −1 V vs SHE.[3,4] This difference can have contributions from the dielectric medium, charge interactions in the vicinity of the site, and hydrogen bonding.

Evidence suggests that the thiolate−Fe bond is highly covalent in these systems, and a modulation of this covalency in the protein could, therefore, contribute to redox properties of the site. Specifically, calculations have been performed on oxidized monomeric iron−sulfur centers and indicate very covalent bonding between the iron and the sulfur.[5−7] These calculations have also shown that, upon reduction, the additional electron density is strongly delocalized onto the ligands. Spectroscopy has shown that the ligand field transitions of $Fe(SR)_4^-$ are ∼1 eV lower in energy than those of $FeCl_4^-$, indicating significant charge-transfer mixing into the d-orbitals, consistent with a highly covalent metal site in the $Fe(SR)_4^-$.[8] Experimentally defining this covalency and its change with hydrogen bonding in the protein is key to understanding this site and defining electronic structure contributions to redox properties and electron-transfer pathways.

The electric dipole-allowed transitions for K-edges are 1s → np. Thus, ligand K-edge X-ray absorption spectroscopy (XAS) provides a direct experimental probe of these ligand−metal bonding interactions. The K-edge absorption of a ligand bound to a d^9 copper ion exhibits a well-defined pre-edge feature which is assigned as a ligand 1s → ψ^* transition, where ψ^* is the half-filled, highest-occupied molecular orbital (HOMO) in Cu(II).[9] Due to the localized nature of the ligand (L) 1s orbital, this transition can have absorption intensity only if the half-filled HOMO orbital contains a significant component of ligand 3p character as a result of covalency. A description of this L 1s → ψ^* transition involves $\psi^* = (1 - \alpha'^2)^{1/2}$[Cu 3d] − α'[L 3p], where α'^2 represents the amount of L 3p character in the HOMO. The observed pre-edge transition intensity is then the intensity of the pure dipole-allowed L 1s → 3p transition weighted by α'^2 (eq 1).

$$I(\text{L 1s} \rightarrow \psi^*) = \alpha'^2 I(\text{L 1s} \rightarrow \text{L 3p}) \qquad (1)$$

Thus, the pre-edge intensity provides a quantitative estimate of the ligand contribution to the HOMO due to bonding.

The pre-edge feature in d^n metal centers other than Cu(II) also corresponds to a transition (or several transitions) from a ligand 1s orbital to unoccupied or partially occupied antibonding

[†] Department of Chemistry, Stanford University.
[‡] University of Georgia.
[§] Stanford Synchrotron Radiation Laboratory, Stanford University.

(1) Day, M. W.; Hsu, B. T.; Joshua-Tor, L.; Park, J.-B.; Zhou, Z. H.; Adams, M. W. W.; Rees, D. C. *Protein Sci.* **1992**, *1*, 1494−1507.
(2) Dauter, Z.; Wilson, K. S.; Sieker, L. C.; Moulis, J.-M.; Meyer, J. *Proc. Natl. Acad. Sci. U.S.A.* **1996**, *93*, 8836−8840.
(3) Holm, R. H.; Kennepohl, P.; Solomon, E. I. *Chem. Rev.* **1996**, *96*, 2239−2314.
(4) Stephens, P. J.; Jollie, D R.; Warshel, A. *Chem. Rev.* **1996**, *96*, 2491−2513.
(5) Norman, J. G., Jr.; Jackels, S. C. *J. Am. Chem. Soc.* **1975**, *97*, 3833−3835.
(6) Bair, R. A.; Goddard, W. A., III. *J. Am. Chem. Soc.* **1978**, *100*, 5669−5676.
(7) Noodleman, L.; Norman, J. G.; Osborne, J. H.; Aizman, A.; Case, D. A. *J. Am. Chem. Soc.* **1985**, *107*, 3418−3426.
(8) Gebhard, M. S.; Deaton, J. C.; Koch, S. A.; Millar, M.; Solomon, E. I. *J. Am. Chem. Soc.* **1990**, *112*, 2217−2231.
(9) Hedman, B.; Hodgson, K. O.; Solomon, E. I. *J. Am. Chem. Soc.* **1990**, *112*, 1643−1645.

10.1021/ja981350c CCC: $15.00
Published on Web 10/03/1998

orbitals with both metal d- and ligand p-character. However, in systems with more than one d-manifold electron or hole, transitions to more than one partially occupied metal d-derived orbital are possible, and multiplet effects in the d^{n+1} final state can affect the observed intensity. Methodology has been developed to analyze these effects for the Cl K-edge pre-edge intensity in a series of tetrahedral metal tetrachlorides, MCl_4^{2-}, where M = Cu(II), Ni(II), Co(II), and Fe(II),[10] and of an analogous series for the S K-edge pre-edge intensity of $M(SR)_4^{2-}$, where M = Ni(II), Co(II), Fe(II), and Mn(II).[11] It is important to note that, in these tetrathiolate complexes, the anisotropy of the thiolate p-orbitals in bonding to the metal has to be taken into account. Based on the MCl_4^{2-} and $M(SR)_4^{2-}$ studies, an expression has been derived for metal centers which allows the ligand HOMO covalency to be quantitatively related to ligand pre-edge intensity.[10,11] This expression for tetrahedral ferric complexes is given in eq 2.

$$D_o(\mathrm{Fe(III)}) = (c_1^2 + c_2^2 + {}^2/_3 c_3^2) R^2 \langle s|\mathbf{r}|p\rangle^2 \qquad (2)$$

D_o is the total experimental intensity, c_1^2 and c_2^2 are coefficients which reflect the ligand 3p σ and π covalency, respectively, in the t_2 set of orbitals, c_3^2 is the coefficient which reflects π covalency in the e set of orbitals, R is the ligand−metal bond distance, and $\langle s|\mathbf{r}|p\rangle^2$ is the intensity of a pure ligand 1s → 3p transition. Thus, ligand K-edge XAS can provide a direct experimental probe of the ligand character in the redox-active orbitals in Fe−S systems.

We have conducted sulfur K-edge XAS studies for a series of rubredoxin proteins and model complexes. S K-edge data of the $Fe^{III}(SR)_4^-$ monomer define the covalency of the thiolate S−Fe(III) bond and provide a reference for ferric tetrathiolate sites in proteins. The S K-edge XAS of an $Fe^{II}(SR)_4^-$ complex has been previously investigated,[11] and it has been observed that there is no pre-edge peak in the sulfur K-edge data that is discernible from the edge. Therefore, comparison of the ferrous and ferric monomers with analogous ligation has allowed us to determine features in the S K-edge spectrum of the ferric monomer and rubredoxin which are assigned as pre-edge transitions. This ferric model complex, which exhibits structural and spectroscopic characteristics very similar to those of the proteins,[12] allows a detailed examination of the electronic structure of the Fe−S active sites. S K-edges of three rubredoxin (Rd) proteins, *Clostridium pasteurianum* (*Cp*), *Pyrococcus furiosus* (*Pf*), and a mutant of the two, which has the first 15 amino acid residues as in *Cp* Rd and the remainder of the protein being the same as *Pf* Rd (*Cp15*|*Pf* Rd), have also been obtained. Comparison of the S K-edges of the model complex and the proteins allows an evaluation of whether hydrogen bonding within the protein site affects the bonding of the thiolate to the ferric center and whether this correlates to redox potentials.

Experimental Section

A. Sample Preparation. The model complexes $Na(Ph_4As)[Fe(o\text{-}C_6H_4(CH_2S)_2)_2]$[13,14] and $[Et_4N][Fe(o\text{-}C_6H_4(CH_2S)_2)_2]$[13,14] as well as the proteins[15] *Pf*, *Cp*, and *Cp15*|*Pf* Rd were prepared according to published procedures. L-Methionine was used as purchased from Sigma Chemical Co.

For the X-ray absorption experiments, the solid samples of model complexes were ground into a fine powder which was dispersed as thinly as possible on Mylar tape to minimize the possibility of self-absorption. The procedure has been verified to minimize self-absorption effects in the data by systematically testing progressively thinner samples until the observed intensity no longer varies with the thickness of the sample. The Mylar tape contained an acrylic adhesive which was determined to have a level of sulfur contaminants below that which is detectable under the conditions of the X-ray absorption measurements. The powder on tape was mounted across the window of an aluminum plate. The samples were prepared in dry, anaerobic atmospheres. A 6.35-μm polypropylene film window protected the solid samples from exposure to air during transfer from a nitrogen-filled glovebox to the experimental sample chamber.

The protein samples were pre-equilibrated in a water-saturated He atmosphere for ∼0.5−1 h to minimize bubble formation in the sample cell. Protein solutions were loaded via syringe into a Pt-coated Al block sample holder sealed in front by a 6.35-μm-thick polypropylene window. The protein concentrations were 2.5, 3.5, and 3.8 mM for *Pf*, *Cp*, and *Cp15*|*Pf* Rd, respectively, in 25 mM tris-HCl buffer at a pH of 8.5. All three protein samples exhibited photoreduction after a few scans and were then reoxidized with approximately 2−3 equiv of a 100 mM solution of $K_3[Fe(CN)_6]$ prepared in deionized water.

B. X-ray Absorption Measurements. X-ray absorption data were measured at the Stanford Synchrotron Radiation Laboratory using the 54-pole wiggler beamline 6-2 in a high magnetic field mode of 10 kG with a Ni-coated harmonic rejection mirror and a fully tuned Si(111) double crystal monochromator, under ring conditions of 3.0 GeV and 50−100 mA. The entire path of the beam was in a He atmosphere. Details of the optimization of this setup for low-energy studies have been described in an earlier publication.[16]

All S K-edge XAS measurements were made at room temperature for the solid samples and at ∼4 °C for the proteins. The data were measured as fluorescence excitation spectra utilizing an ionization chamber as a fluorescence detector.[17,18] To check for reproducibility, at least 2−3 scans were measured for each solid sample, while multiple scans were measured for the proteins to obtain a good signal-to-noise level in the data and to monitor photoreduction of the samples. The final averages for the proteins were based on two, four, and three scans for the *Pf*, *Cp*, and *Cp15*|*Pf* Rd, respectively. The energy was calibrated from the S K-edge spectra of $Na_2S_2O_3{\cdot}5H_2O$ which were collected at intervals between the samples. The maximum of the first pre-edge feature in the spectrum was assigned to 2472.02 eV. Scans ranged from 2420 to 2740 eV and from 2440 to 2525 eV for models and proteins, respectively, with a step size of 0.08 eV in the edge region. The spectrometer energy resolution was ∼0.5 eV.[16] Calculating and comparing first and second derivatives for model compounds measured repeatedly during different experimental sessions results in a reproducibility in edge position of ∼0.1 eV for these experiments.

C. Data Reduction. Data were averaged and a smooth background was removed from all spectra by fitting a polynomial to the pre-edge region and subtracting this polynomial from the entire spectrum. Normalization of the data was accomplished by fitting a flat polynomial or straight line to the postedge region and normalizing the edge jump to 1.0 at 2490 eV. A figure depicting full scans of the normalized data is included as Supporting Information to illustrate the utility of the normalization process.

D. Fitting Procedures. The intensities of pre-edge features of the blue copper protein plastocyanin,[19] the ferric model complexes, and

(10) Shadle, S. E.; Hedman, B.; Hodgson, K. O.; Solomon, E. I. *J. Am. Chem. Soc.* **1995**, *117*, 2259−2272.
(11) Rose Williams, K.; Hedman, B.; Hodgson, K. O.; Solomon, E. I. *Inorg. Chim. Acta* **1997**, *263*, 315−321.
(12) Holm, R. H.; Berg, J. M. In *Iron−Sulfur Proteins*; Spiro, T. G., Ed.; John Wiley & Sons: New York, 1982; pp 1−66.
(13) Lane, R. W.; Ibers, R. A.; Frankel, R. B.; Holm, R. H. *Proc. Natl. Acad. Sci. U.S.A.* **1975**, *72*, 2868−2872.
(14) Lane, R. W.; Ibers, J. A.; Frankel, R. B.; Papaefthymiou, G. C.; Holm, R. H. *J. Am. Chem. Soc.* **1977**, *99*, 84−98.
(15) Eidsness, M. K.; Richie, K. A.; Burden, A. E.; Kurtz, D. M., Jr.; Scott, R. A. *Biochemistry* **1997**, *36*, 10406−10413.
(16) Hedman, B.; Frank, P.; Gheller, S. F.; Roe, A. L.; Newton, W. E.; Hodgson, K. O. *J. Am. Chem. Soc.* **1988**, *110*, 3798−3805.
(17) Lytle, F. W.; Greegor, R. B.; Sandstrom, D. R.; Marques, E. C.; Wong, J.; Spiro, C. L.; Huffman, G. P.; Huggins, F. E. *Nucl. Instrum. Methods* **1984**, *226*, 542−548.
(18) Stern, E A.; Heald, S. M. *Rev. Sci. Instrum.* **1979**, *50*, 1579−1582.
(19) Shadle, S. E.; Penner-Hahn, J. E.; Schugar, H. J.; Hedman, B.; Hodgson, K. O.; Solomon, E. I. *J. Am. Chem. Soc.* **1993**, *115*, 767−776.

the rubredoxins were quantified by fits to the data. The fitting program EDG_FIT, which utilizes the double precision version of the public domain MINPAK fitting library,[20] was used. EDG_FIT was written by Dr. Graham N. George of the Stanford Synchrotron Radiation Laboratory. Pre-edge features were modeled by pseudo-Voigt line shapes (simple sums of Lorentzian and Gaussian functions). This line shape is appropriate as the experimental features are expected to be a convolution of the Lorentzian transition envelope[21] and the Gaussian line shape imposed by the spectrometer optics.[17,22,23] A fixed 1:1 ratio of Lorentzian to Gaussian contribution for the pre-edge feature successfully reproduced these spectral features. The rising edge functions were also pseudo-Voigt line shapes for which the Gaussian: Lorentzian mixture was allowed to vary to give the best empirical fit. Good fits which were used in the calculation of pre-edge peak intensity were those which were optimized to reproduce both the data and the second derivative of the data using a minimum number of peaks. Based on a pre-edge peak half-width range of 0.5−0.6 eV, one to three peaks were used to reasonably fit the pre-edge feature of the data, and a number of good fits were obtained for each spectrum. It should also be noted that a four-peak theoretical fit of the pre-edge of $[Et_4N][Fe(o\text{-}C_6H_4(CH_2S)_2)_2]$ (vide infra) was performed to illustrate d-orbital splitting but was not used in the final calculation of covalency for that complex. Fits were performed over several energy ranges: from one which included just the tail of the rising edge to one which included the white line maximum of the edge. The intensity of a pre-edge feature (where peak intensity was approximated by peak area, calculated as the height times full-width-at-half-maximum) is the sum of the intensities of all the pseudo-Voigts which successfully fit the feature for a given fit. The final reported intensity values were calculated by averaging all of the good pre-edge fits, which include from one to three functions in the pre-edge region, for both the model complex and the proteins. It should be noted that, since similar pre-edge intensities were obtained using from one to three features in the pre-edge region and reasonable half-widths were used for all fits, it was proper to include all of these fits in the final intensity average.

E. Error Sources and Analysis. There are several possible sources of systematic error in the analysis of these spectra. Normalization procedures can introduce a 1−3% difference in pre-edge peak heights, as determined by varying the parameters used to normalize a set of Cl K-edge spectra such that the final fits met requirements of consistency. For each sample, the standard deviation of the average of the pre-edge areas for the acceptable series of fits described in the previous section was calculated to quantitate the uncertainty of the fit. This maximum of ∼3% normalization error and the error resulting from the fitting procedure were combined and reported along with the determined covalency values in the following Results and Analysis section. The uncertainty in pre-edge energies is limited by the reproducibility of the edge spectra (∼0.1 eV). Thus, energies of features are reported with an error of ±0.1 eV.

Results and Analysis

The S K-edge XAS spectra of the ferric model complex ($[Et_4N][Fe(o\text{-}C_6H_4(CH_2S)_2)_2]$) along with that of its ferrous analogue ($(Na(Ph_4As)[Fe(o\text{-}C_6H_4(CH_2S)_2)_2]$) are shown in Figure 1. Since both complexes have open d-shells, they can exhibit pre-edge features in the S K-edge spectrum. Comparison of the ferric complex data with the ferrous complex data, however, shows a feature at ∼2470 eV present only in the spectrum of the ferric complex. As previously determined,[11] ferrous tetrathiolate model complexes do not display a pre-edge feature that is lower in energy than the edge. Therefore, the feature observed in the pre-edge region of the S K-edge spectrum of the ferric complex is assigned as the S 1s → S 3p transition and reflects the fact that the metal 3d mixes significantly with the S 3p orbitals in these ferric complexes. The greater effective nuclear charge of the ferric versus the ferrous site shifts the pre-edge feature in the ferric complex to lower energy since the metal d-orbitals are at deeper binding energy and, therefore, closer in energy to the S 1s orbital. This difference in ferric versus ferrous d-orbital energy results in a pre-edge feature that is discernible from the edge feature in the ferric complex.

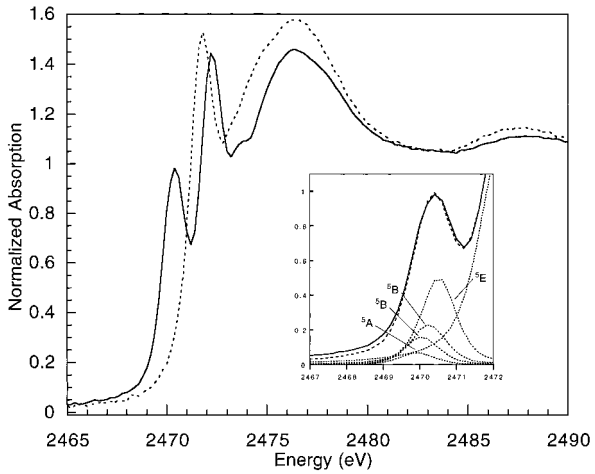

Figure 1. S K-edge XAS spectra of $Fe(o\text{-}C_6H_4(CH_2S)_2)_2^-$ (—), and $Fe(o\text{-}C_6H_4(CH_2S)_2)_2^{2-}$ (- - -). The inset shows the pre-edge region of the $[Et_4N][Fe(o\text{-}C_6H_4(CH_2S)_2)_2]$ S K-edge spectrum and includes a representative four-peak fit performed based on the d-orbital splitting diagram of Gebhard et al.[8] (Figure 16 in that reference) with a 20% reduction in the splitting based on the effects of a core hole in the d-manifold in XAS. Each of the four peaks in the fit is labeled as the d^{n+1} parent state based on an electronic transition to the corresponding orbital. The fit from the four peaks in the inset is represented with the dashed line, while the data are represented by the solid line.

The intensity of this ligand pre-edge feature can be related to the metal−ligand covalency. To determine the metal−ligand covalency in the ferric tetrathiolate complex and the proteins, the intensity of the pre-edge feature of the well-understood blue copper protein, plastocyanin, is used as the reference. For plastocyanin, this pre-edge feature has an intensity of 1.02 units, which corresponds to a covalency of 38% S−Cys in the Cu−S bond.[19] Since this intensity is normalized to one sulfur, the intensity of the ferric tetrathiolates needs to be multiplied by a factor of 4 for comparison to blue copper. Also, bond length and effective nuclear charge differences between the Cu and Fe complexes need to be taken into account when calculating the total covalency (eq 2). While the bond length difference is significant and has an effect on the quantification of the covalency, it has been previously determined that the effective nuclear charge difference between the Cu(II) and the Fe(III) is negligible.[10] The inclusion of the bond length differences $((R_{Cu}/R_{Fe})^2$ in eq 2, where R_{Cu} is 2.13 Å[24] and R_{Fe} is 2.27[14]Å) indicates that the $[Et_4N][Fe(o\text{-}C_6H_4(CH_2S)_2)_2]$ S K-edge pre-edge feature, which has an intensity of 1.15, corresponds to a total Fe−S covalency of 151 ± 8% over the five half-occupied d-orbitals as shown in Table 1.

The inset of Figure 1 contains the S K-edge spectrum of $[Et_4N][Fe(o\text{-}C_6H_4(CH_2S)_2)_2]$ and a representative fit to the data. In the approximate S_4 symmetry of the $Fe(SR)_4^-$ model complex, the e and t_2 orbitals (separated by 10 *Dq* in T_d symmetry) split further into a and b and b and e levels, respectively. Transitions to these four levels (a, b, b, and e)

(20) Garbow, B. S.; Hillstrom, K. E.; More, J. J. *MINPAK*; Argonne National Laboratory: Argonne, IL, 1980.
(21) Agarwal, B. K. *X-ray Spectroscopy*; Springer-Verlag: Berlin, 1979.
(22) Lytle, F. W. In *Applications of Synchrotron Radiation*; Winick, H., Xian, D., Ye, M. H., Huang, T., Eds.; Gordon & Breach: New York, 1989; p 135.
(23) Tyson, T. A.; Roe, A. L.; Frank, P.; Hodgson, K. O.; Hedman, B. *Phys. Rev. B* **1989**, *39A*, 6305−6315.
(24) Guss, J. M.; Freeman, H. C. *J. Mol. Biol.* **1983**, *169*, 521−563.

Table 1. S K-Edge Intensities and Covalencies

sample	normalized pre-edge intensity	renormalized pre-edge intensity[a]	rescaled total S covalency (%)[b]
$[Et_4N][Fe(o-C_6H_4(CH_2S)_2)_2]$	1.15	1.15	151 ± 8
Pf Rd	0.96	0.96	125 ± 6
Cp Rd	0.83	1.03	135 ± 8
*Cp*15|*Pf* Rd	0.79	0.98	129 ± 7

[a] Renormalized pre-edge intensity is based on the ratio of the total number of sulfurs to the number of sulfurs bound to the Fe that contribute to pre-edge intensity. [b] Total S covalency is based on a comparison of intensities to that of Pc in which one Cu−S has an intensity of 1.02 normalized absorption units and a covalency of 38%. This value is then multiplied by 4 to account for the four thiolate groups. The total sulfur covalency is based on differences in Fe−S and Cu−S bond lengths. Therefore, the final value is rescaled by $(2.13 \text{ Å}/ 2.27 \text{ Å})^2$.

correspond to transitions to ^{5}A, ^{5}B, ^{5}B, and ^{5}E d^{n+1} parent states. Therefore, it is expected that four peaks could potentially be observed in the pre-edge feature of the S K-edge spectrum of $[Et_4N][Fe(o\text{-}C_6H_4(CH_2S)_2)_2]$. Such a fit was performed using four peaks to represent the d-orbital splittings and to investigate relative contributions of covalency and allow for a comparison of σ versus π covalency. This fit, shown in the inset of Figure 1, had peak energy splittings based on the d-orbital splitting diagram of an S_4 $Fe(SR)_4^-$ model complex observed by Gebhard et al.[8] from polarized single-crystal absorption and magnetic circular dichroism. This energy of the d-orbital splitting was reduced by 20% to account for the fact that the d-manifold more closely resembles a d^6 configuration in the final state and this configuration typically has a reduced ligand field orbital splitting pattern for a complex with the same ligation. The intensities of the features of this four-peak fit were designated on the basis of the fact that d-orbitals higher in energy will have higher covalency. Therefore, it is expected that the intensities of these features resulting from transitions to parent states will vary by $^5A < {}^5B < {}^5B < {}^5E$. In addition, the intensity of the feature from the transition to the ^{5}E parent state will have at least twice the covalency of the transition to the highest energy ^{5}B parent state since the ^{5}E is based on a doubly degenerate d-orbital. Shown is a representative fit designed to maximize the two lowest energy peaks to determine the maximum possible π covalency in the complex. It was found that the π covalency was a maximum of 30% of the σ content, which was represented by the other two higher energy peaks of the fit. It should be noted that four peaks are not observed in the second derivative of the data due to the closeness in energy of the peaks and the spectral bandwidth of the experiment ($\sim$0.5 eV).

The S K-edge XAS spectra of the three ferric rubredoxins, *Pf* Rd, *Cp* Rd, and *Cp15*|*Pf* Rd, are shown in Figure 2. Edge and pre-edge energies are similar for the three proteins, indicating that the core 1s energy of the S orbitals and the ligand field splitting are very similar. In addition to the four S−Cys present in the active site of the proteins, the *Cp* Rd and *Cp15*|*Pf* Rd contain an additional N-terminal methionine residue. This additional sulfur accounts for the difference in the S K-edge spectrum observed in Figure 2. In the region just above the edge at $\sim$2474 eV, the spectra of the *Cp* Rd and *Cp15*|*Pf* Rd have higher intensities than that of *Pf* Rd. This 2474-eV feature is comparable to a feature in this region of the S K-edge spectrum of pure L-methionine, also shown in Figure 2. Since the *Cp* Rd and *Cp15*|*Pf* Rd have five sulfurs that contribute to the edge, but only four that contribute to the pre-edge feature (only those sulfurs bound to the iron atom contribute to pre-edge intensity), these data have been renormalized by a factor of 5/4, and the pre-edges are shown in the inset of Figure 2

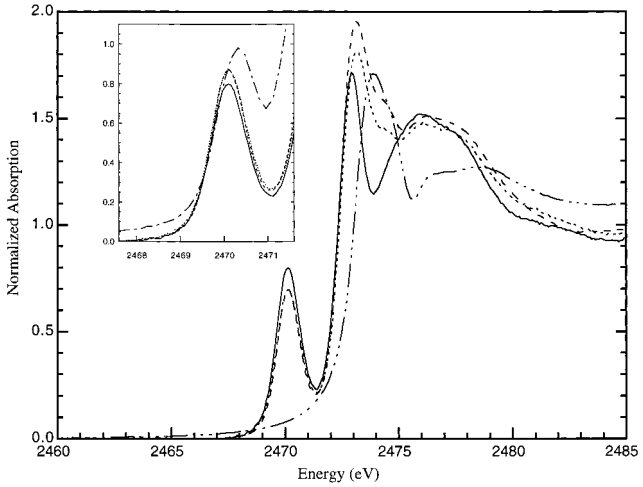

Figure 2. S K-edge XAS spectra of *Pf* Rd (—), *Cp* Rd (···), *Cp15*|*Pf* Rd (---), and L-methionine (— ··· —). The S K-edge of L-methionine is shown to illustrate differences in edge structure due to the presence of a S−Met in the *Cp* and *Cp15*|*Pf* Rd. The inset shows the renormalized pre-edge data for the three proteins and also the $[Et_4N][Fe(o\text{-}C_6H_4(CH_2S)_2)_2]$ (— · —) model complex data for comparison.

along with those of *Pf* Rd and the $[Et_4N][Fe(o\text{-}C_6H_4(CH_2S)_2)_2]$ model complex. The fit intensities of these renormalized features are 0.96, 1.03, and 0.98 for the *Pf* Rd, *Cp* Rd, and *Cp15*|*Pf* Rd, respectively, corresponding to total S−Cys−Fe covalencies (obtained as discussed above for $[Et_4N][Fe(o\text{-}C_6H_4(CH_2S)_2)_2]$) of $125 \pm 6\%$, $135 \pm 8\%$, and $129 \pm 7\%$,[25] as shown in Table 1.

Discussion and Conclusion

The total covalency of the $[Et_4N][Fe(o\text{-}C_6H_4(CH_2S)_2)_2]$ model complex is $151 \pm 8\%$. SCF-Xα-SW calculations with spheres adjusted to reproduce spectral data[26] give a total covalency of 140% for a tetrathiolate monomer. Therefore, the experimental covalency is in reasonable agreement with the calculations. It should be noted, however, that the calculations overestimate π covalency. As shown in the inset of Figure 1, representing a fit maximizing the two lowest energy π peaks, the maximum π contribution to covalency is $< 30\%$, whereas the calculations give a π covalency of $\sim$45%. This overestimation is consistent with the charge-transfer analysis performed by Gebhard et al.,[8] where $\pi \rightarrow \pi$ charge-transfer intensity is very weak, but $\sigma \rightarrow \sigma$ charge-transfer intensity is strong.

The intensities of the S K-edge pre-edge feature of the proteins are lower than that of the $[Et_4N][Fe(o\text{-}C_6H_4(CH_2S)_2)_2]$ model (maximally, 26% lower). The most significant structural difference between the model and protein sites is that the model sites do not contain hydrogen bonds, whereas all three protein sites have six N−H···S hydrogen bonds from backbone residual donors to the thiolate-S.[1,2,27] The average N−H···S distance is 3.50, 3.63, and 3.62 Å in *Pf*, *Cp*, and *Cp15*|*Pf* Rd, respectively. Hydrogen bonding from the protein amino acids to the coordinated thiolates should cause a decrease in the sulfur charge donation to the metal ion, and thus a decrease in thiolate−Fe covalency, which is observed. This covalency difference could be due to variations in the strength and orientation of the specific hydrogen bonds. It could also be

(25) Since the bond lengths of these complexes are similar based on these crystal structures[1,2,27] and EXAFS,[28,29] the same ratio was used for R_{Fe} in the comparison with R_{Cu} for all of the proteins.

(26) Guckert, J. A. Ph.D. Thesis, Stanford University, Stanford, CA, 1995.

(27) Kang, C. H.; Eidsness, M. K.; Kurtz, D. M., Jr.; Scott, R. A. unpublished results.

due to the fact that the number of hydrogen bonds in the β-sheet region is 9, 7, and 5 for *Pf*, *Cp*, and *Cp15|Pf* Rd, respectively. β-Sheet strands 1 and 2 form the stem of a loop that provides two of the cysteinyl ligands to Fe, suggesting a more rigid framework with increasing number of hydrogen bonds, which could have an effect on the Fe−S centers.

Changes in covalency of the ligand−metal bonds should contribute to the redox properties of an active site. A reduction in covalency of the thiolate−Fe bond should lead to a higher effective nuclear charge on the metal ion. The larger the effective nuclear charge, the more the potential is expected to increase.[3] Indeed, the proteins are generally less covalent and have higher reduction potentials than the model complexes by about 1 V. However, in the rubredoxins, the protein potentials follow the order *Cp*, *Pf*, and *Cp15|Pf* Rd and are −60, +5, and +69 mV, respectively.[3,4,28] While the protein with the highest covalency (*Cp* Rd) also has the lowest reduction potential, there is no systematic trend since the covalencies are essentially the same for the other two proteins. Also, the reduction in covalency is over 1.5 times larger in *Pf* than in *Cp* as compared to the model complex, yet the potential changes by only 65 mV. Since the ligand K-edge spectroscopy is a direct probe of covalency, and there is a difference in covalency between the model and the proteins, but no significant correlation between the potentials and the change in covalency, it is reasonable to conclude that other protein factors make dominant contributions to the generally higher redox potentials of the rubredoxin sites.

Ligand K-edge spectroscopy provides an experimental probe of covalency in open-shell metal ions. We have used S K-edge spectroscopy to investigate the thiolate−Fe covalency in the $Fe(SR)_4^-$ site of a model complex and in a series of rubredoxins. This is the first example of the application of using this S K-edge methodology to understand covalency in iron−sulfur proteins. Our results show that the thiolate−Fe covalency is higher for the model complex than it is for the rubredoxin sites, which is consistent with the expected effects of hydrogen bonding. S K-edge XAS produces a quantitative evaluation of these covalency and hydrogen bonding effects. There is neither a strong correlation of the changes in covalency with hydrogen bonding nor with the redox potentials of the $Fe(SR)_4^-$ sites, indicating that other contributions from the protein environment, such as dielectric medium and charge interactions, likely dominate. This study assays the pre-edge region of the S K-edge of an iron system and provides the basis for the future investigation of covalency in other iron−sulfur sites containing multiple iron centers.

Acknowledgment. This research was supported by NSF CHE-9528250 (E.I.S.) and CHE-9423181 (K.O.H.) and by NIH RR-01209 (K.O.H.). Stanford Synchrotron Radiation Laboratory operations are funded by the Department of Energy, Office of Basic Energy Sciences. The Biotechnology Program is supported by the National Institutes of Health, National Center for Research Resources, Biomedical Technology Program, and by the Department of Energy, Office of Biological and Environmental Research. Further support was provided by grants from the National Institutes of Health (GM50736) and the National Science Foundation Research Training Group Award to the Center for Metalloenzyme Studies (DIR 90-14281).

Supporting Information Available: Figure containing full scans of the normalized S K-edge data of the $[Et_4N][Fe(o\text{-}C_6H_4(CH_2S)_2)_2]$ and the rubredoxin proteins (1 page, print/PDF). See any current masthead page for ordering information and Web access instructions.

JA981350C

(28) Eidsness, M. K.; Smith, E. T.; Kurtz, D. M., Jr.; Scott, R. A. unpublished results.

(29) George, G. N.; Pickering I. J.; Prince, R. C.; Zhou, Z. H.; Adams, M. W. W. *J. Biol. Inorg. Chem.* **1996**, *1*, 226−230.